Temperature effect on the optical emission intensity in laser induced breakdown spectroscopy of super alloys

S. M. R. Darbani Faculty of Science, Department of Physics, University of Isfahan, Isfahan, Iran

M. Ghezelbash Optics & Laser Science and Technology Research Center, Malek Ashtar University of Technology, Isfahan, Iran

A. E. Majd Electrical Engineering & Electronic Department, Malek Ashtar University of Technology, Tehran, Iran

M. Soltanolkotabi soltan@sci.ui.ac.ir Faculty of Science, Department of Physics, University of Isfahan, Isfahan, Iran

H. Saghafifar Optics & Laser Science and Technology Research Center, Malek Ashtar University of Technology, Isfahan, Iran

In this paper, the influence of heating and cooling samples on the optical emission spectra and plasma parameters of laser-induced breakdown spectroscopy for Titanium 64, Inconel 718 super alloys, and Aluminum 6061 alloy is investigated. Samples are uniformly heated up to approximately 200°C and cooled down to -78°C by an external heater and liquid nitrogen, respectively. Variations of plasma parameters like electron temperature and electron density with sample temperature are determined by using Boltzmann plot and Stark broadening methods, respectively. Heating the samples improves LIBS signal strength and broadens the width of the spectrum. On the other hand, cooling alloys causes fluctuations in the LIBS signal and decrease it to some extent, and some of the spectral peaks diminish. In addition, our results show that electron temperature and electron density depend on the sample temperature variations.
[DOI: http://dx.doi.org/10.2971/jeos.2014.14058]

Keywords: Laser-induced breakdown spectroscopy (LIBS), temperature, titanium 64, inconel 718, aluminum 6061

1 INTRODUCTION

Laser-Induced Breakdown Spectroscopy (LIBS) is an analytical technique for determination of elemental composition of materials (solid, liquid, and gas). The main features of LIBS are: no initial sample preparation, low consumption of sample, simultaneous multi elemental monitoring, fast detection, non-destructive aspect, on-line and *in situ* [1, 2]. In this technique, plasma plume is produced by focusing the pulsed laser on the sample surface. The intensities, which are high enough to result in plasma formation through the subsequent process of vaporization and atomization in a single step, are involved in the $GWcm^{-2}$ range for the nanosecond duration. This plume consists of atoms, ions, and free electrons. Free electrons absorb energy from the laser pulse and transfer it to the atoms and ions by collisions. Consequently, more electrons are created through ionization process [3]. The emitted light of LIBS consists of discrete lines and a continuum background. These discrete lines characterize the materials. The discrete emission lines from the atomic species can be hidden by continuum radiation caused by two processes: recombination radiation and bremsstrahlung processes [4, 5].

Increasing the signal intensity is important in LIBS technique. In most studies, several methods like Time Resolved LIBS (TR-LIBS) [6], Spatial Resolved LIBS (SRLIBS) [7], Polarization Resolved LIBS (PRLIBS) [8, 9], Dual Pulse LIBS [10], applying electric and magnetic fields [11] , and combination of the Ultra Violet (UV) and Near Infrared (NIR) pulses [12] have been used for this purpose. Initial temperature variation of sample might be another method discussed in this paper. To the best of our knowledge, a few reports exist in regard to sample temperature variations in order to improve LIBS signal, mainly due to the preheating process. Tavassoli et al. [13] reported the effect of initial sample temperature on spectral emission LIBS for aluminum alloy surface at ambient air pressure. The sample is uniformly heated up to 150°C and the results suggest that increasing the sample temperature can improve the Limits of Detection (LOD). The effect of sample temperature on femtosecond signal pulse LIBS has been reported in [14]. Su et al. [15] showed that heating glass samples could improve SNR. The effects of sample temperature on LIBS signals for stainless steel samples are shown in [16]. Sangines et al. [17] studied the effect of sample temperature on the emission line intensification mechanisms in orthogonal dual- pulse LIBS. The effect of sample temperature and physical state on LIBS spectra of molten and solid salts has been investigated in [18]. Eschlbock-Fuchs et al. studied the influence of sample temperature on the dynamics and optical emission of Laser-Induced Plasma (LIP) for aluminum alloy, silicon wafer, and metallurgical slag samples [19]. Shoursheini et al. have investigated the enhancement of Cu emission lines of a micro-plasma induced by a Nd:YAG laser due to the thermal effect of simultaneous irradiation by a continuous wave CO_2 laser [20].

Received September 08, 2014; resubmitted November 13, 2014; published December 22, 2014 ISSN 1990-2573

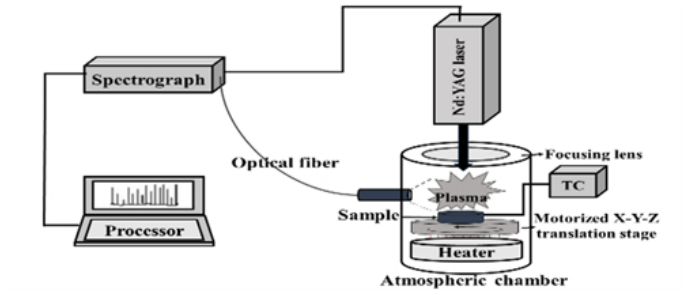

FIG. 1 Schematic diagram of the experimental LIBS set-up.

In this work, we study the influence of heating and cooling the samples on optical emission intensity in Laser-Induced Breakdown Spectroscopy spectra in Titanium 64, Inconel 718 super alloys, and aluminum 6061 alloy. The electron temperature and the electron density are determined by using Boltzmann plot method and Stark broadening, respectively. The Validity of the Local Thermodynamic Equilibrium (LTE) assumption is shown by the McWhirter criterion.

2 EXPERIMENTAL SET-UP

The experimental set-up is shown in Figure 1. All samples were irradiated with a 100 mJ, 7±2ns pulse width, and 1064 nm wavelength produced by a Q-Switched Nd:YAG laser (ULTRA Laser, Quantel). Maximum laser irradiance on the sample was up to 2 GW/cm^2. The Samples were placed on X, Y, Z motorized translation stage controlled by internal software (LIBSoft V9. 0. 9, Applied Photonic Ltd) that enables precise adjustment of the detection system with respect to the ablation plume. Alloy samples were uniformly heated by an external heater, up to 200°C and were cooled by liquid nitrogen down to (-78°C). In both cases, the sample temperatures were measured by a Thermo Couple (TC) (TC4Y-14R, Autonics) system that can record temperature variations from (-100) to 400°C with 1°C accuracy. An optical system that collects the emitted light from the sample and transmits it to the spectrometer is located perpendicularly at the distance of approximately 3 mm above the sample. The spectrometers (Avantes -29-01-13-A, Netherland) can give 0.04 nm resolution for spectral analysis from 182 to1057 nm. The detector was triggered ∼5 µs after the onset of the laser shot in order to reduce the continuum background radiation. The LIBS spectrum is analyzed by Plasus Specline software (Plasus, Germany).

3 RESULTS AND DISCUSSION

3.1 Heating Sample

Titanium 64, Inconel 718 super alloy, and Aluminum 6061 alloy were chosen as the target samples. The spectra of these alloys were recorded with respect to variations of sample temperature. The selected lines are 396.15 nm, 422.74 nm, 589.04 nm of Al I, Al II, and Fe I, respectively. The mean of ten subsequent spectra is taken into account for the analysis. Figure 2 shows the variation of LIBS signal with sample temperature at different neutral and ionic lines. The intensity of an emission line reported in reference [21], is proportional to the

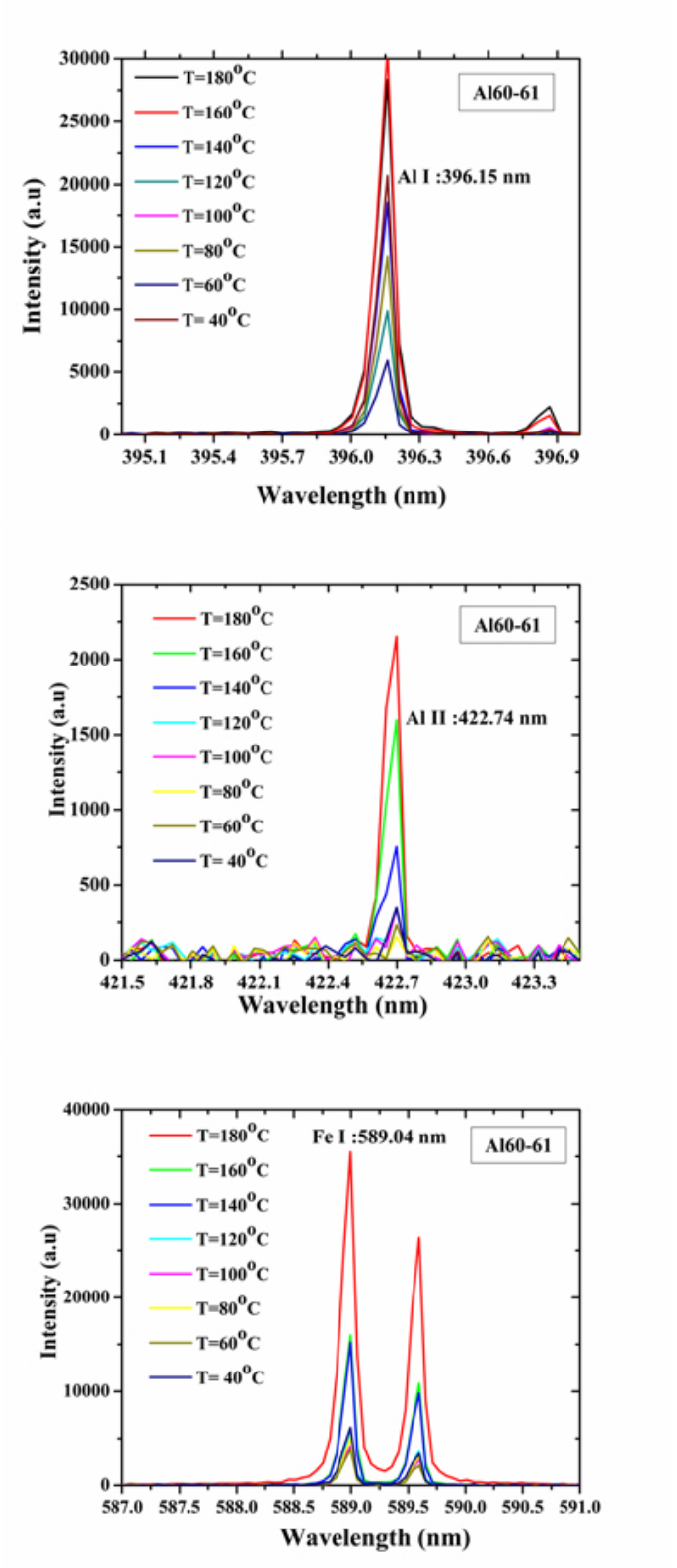

FIG. 2.1 Emitted intensity as a function of wavelength in Al6061 sample. Temperature interval is 40-180°C.

total ablated mass of the plasma constituents. Higher ablation rates at high temperatures of all samples caused this effect. The total ablated mass from target depends on many parameters like specific heat and partial reflectivity of the sample surface. The maximum amount of material M that could be vaporized is given by [22].

$$M = \frac{E_c}{C_p(T_b - T) + l} \quad (1)$$

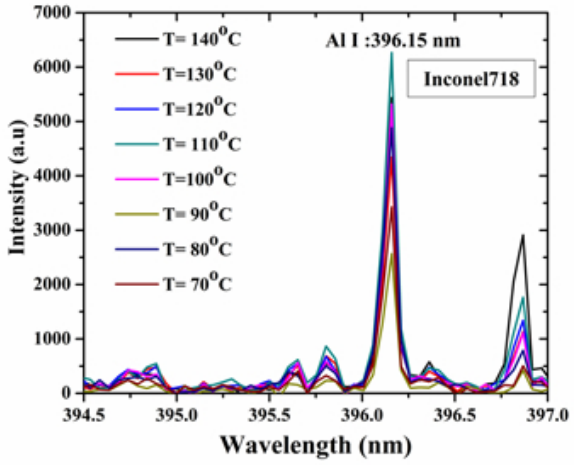

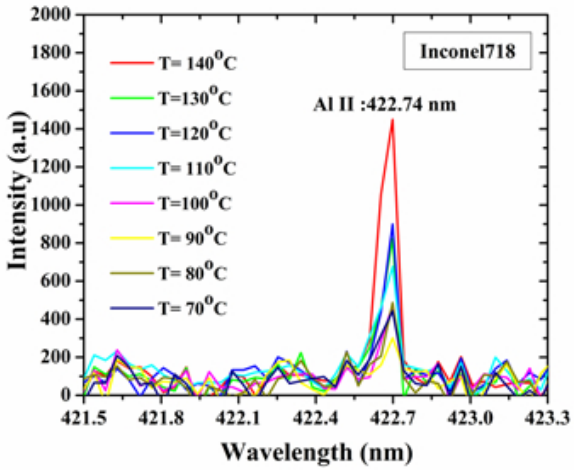

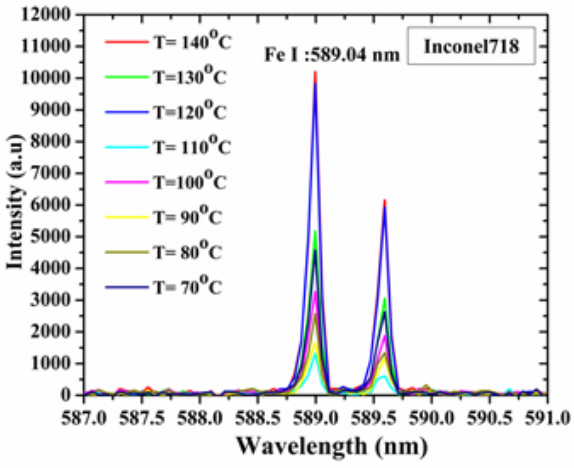

FIG. 2.2 Emitted intensity as a function of wavelength in In718 sample. Temperature interval is 70-140°C.

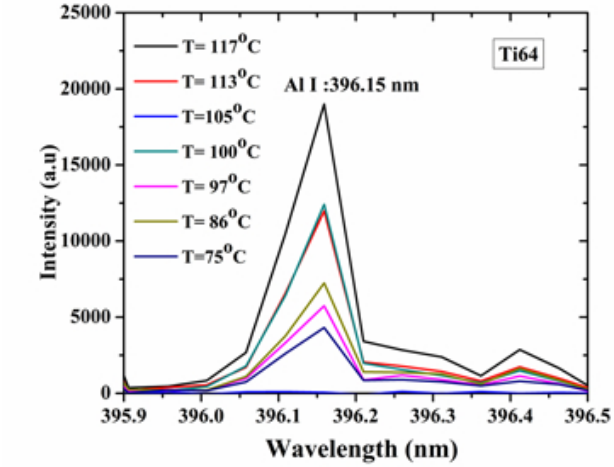

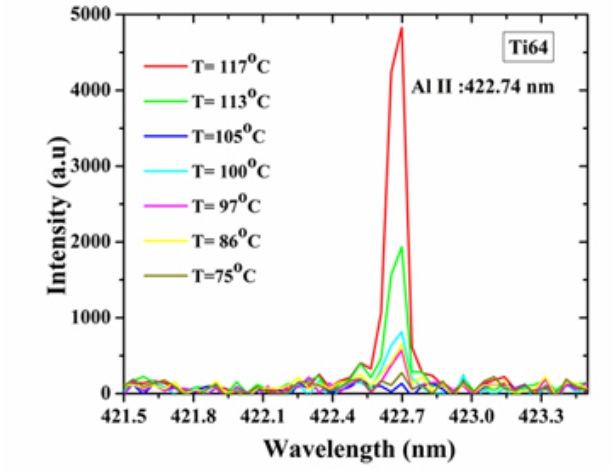

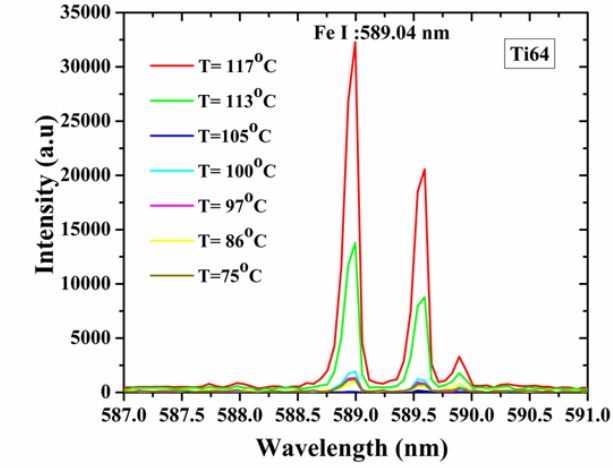

FIG. 2.3 Emitted intensity as a function of wavelength in Ti64 sample. Temperature interval is 75-117°C.

Where, $E_c = E\,[1 - R(T)]$ represents the laser energy coupled to the sample and E, C_p, T_b, l and T denote the energy per pulse, specific heat, boiling temperature, the latent heat, and the initial temperature of the sample, respectively. The melting point of Al6061, In718, and Ti64 correspond to 582^{o}C, 1260^{o}C, and 1604^{o}C, respectively [23]. These melting points are far beyond the temperature variation range (T~200^{o}C) applied to the samples. The partial reflectivity of the target determines the fraction of the coupled laser energy. The reflectivity of metal generally decreases with increasing temperature. This behavior in many metals can be described to a good approximation by the linear relationship [24]:

$$R(T) = R_0 - R_1(T - T_0) \qquad (2)$$

Where, $R_0 = R\,(T_0)$, T_0 is room temperature and R_1 is a constant. The partial reflectivity at 1.06 μm of AL6061, In718, and

Ti6061 correspond to 0.94, 0.72, and 0.57, respectively [25]. As can be seen from Eq. (1) and (2), the maximum amount of ablated materials (M) significantly increases with partial reflectivity during increasing the sample temperature. The effect of sample temperature on the LIBS process evaluated via heating target in different samples is shown in Figure 3. The neutral and ionic transitions remained approximately constant, for T values up to 150, 130, and 200°C in In718, Ti64, and Al6061, respectively. This figure shows the enhancement of intensity with increasing sample temperature for both ionic and atomic lines in all samples. From Eq. 1, we see that for high value of E_c, we obtained the higher ablated mass M, that indicates the lower value of R(t). According to Eq. (2) for lower value of R(t), we have to have higher value of R_1 (for a given temperature) which means sample of higher reflectivity such as Al gives off more LIBS signal intensity as shown in Figure 2. In this situation, the amount of vaporized material available for excitation also increases, leading to the higher amplitude of the characteristic peaks. This result is similar to that reported by [17] for Al samples.

3.2 Cooling Sample

The spectral emission lines of Al6061 in different cooling temperatures have been shown in Figure 4. Here, we considered the LIBS signal after applying first 10 laser shots to remove the surface ice completely. With regard to the fact that at low temperatures, a film of ice is formed on the sample surface. First, this film should be removed and then LIBS signal is recorded. For this reason, LIBS signal is not recorded in the first few laser pulses, so that the surface of the ices is completely removed. In this situation, the spectrum has a fluctuation behavior and damping of some peaks that lead to an important loss of analytical information. These results are similar to what is given by Salle et al. in regard to simulated Martian atmosphere [26]. With further sample cooling, we obtain a reduced wavy signal, which is hard to get any information. This behavior is very clear in atomic lines. The spectra of In718 and Ti64 super alloys have similar behaviors too. The intensity of their fluctuation lines is higher than Al6061 alloy line intensity. Figure 5 shows the effect of sample cooling on LIBS signals. A comparison of spectra obtained at the temperatures of 70°C and (-70°C) is shown in Figure 6. It is clear that measurement at low temperatures leads to an important loss of analytical information. As an example, the Al (II) peak at 867.12 nm at positive temperature exists, but in cooling process, this peak is lost. It seems that the observed signal reduction for temperatures below zero is mainly related to the decrease in the ablation rate [26]. A signal reduction to about 13% was observed in (-70) °C with respect to 70°C surface temperature.

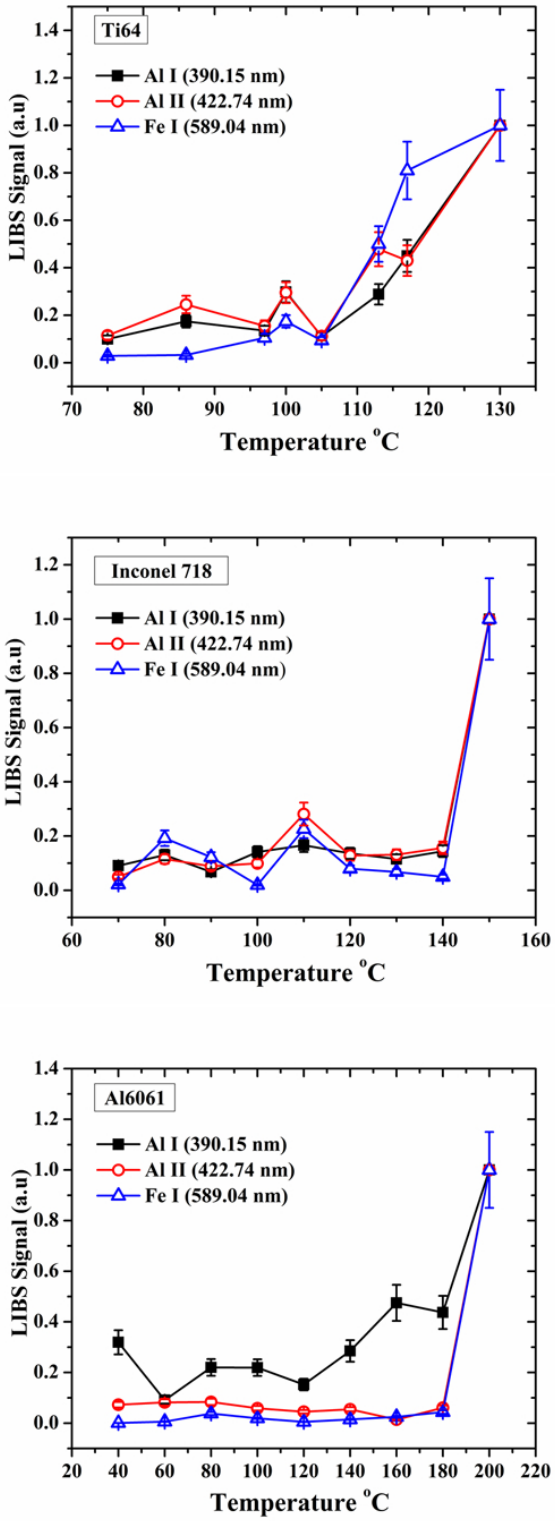

FIG. 3 Emitted intensity of spectral peaks as a function of the sample temperature.

3.3 Plasma characterization

The Boltzmann plot method and the Local Thermodynamic Equilibrium (LTE) assumption are used for the determination of electron temperature and electron density. The Boltzmann equation used for the determination of these parameters is given by [27]:

$$ln\frac{I_{mn}}{g_m A_{mn}} = ln\frac{N(T)}{U(T)} - \frac{E_m}{KT} \quad (3)$$

Where, m, n, I_{mn}, g_m, and A_{mn} are an upper level, lower level, the line intensity, level degeneracy, and the transition probability, respectively. $N(T)$, $U(T)$, E_m, K, and $T$are the number of species, the partition function, the upper energy level, the Boltzmann constant, and the electron temperature, respectively. The spectroscopic parameters of selected spectral lines in this work have been derived from the available atomic spectra database [28, 29] and are summarized in Table 1. The electron temperature can be obtained from the slope of line

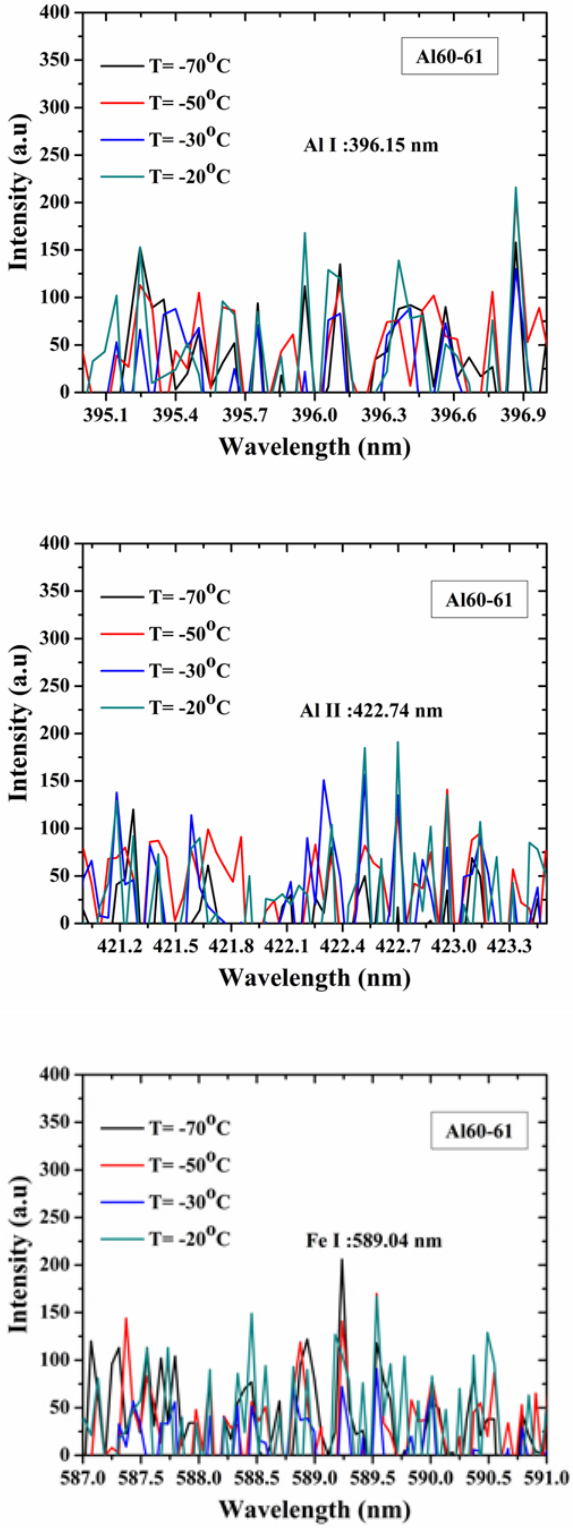

FIG. 4 Emitted intensity of spectral peaks as a function of the sample temperature.

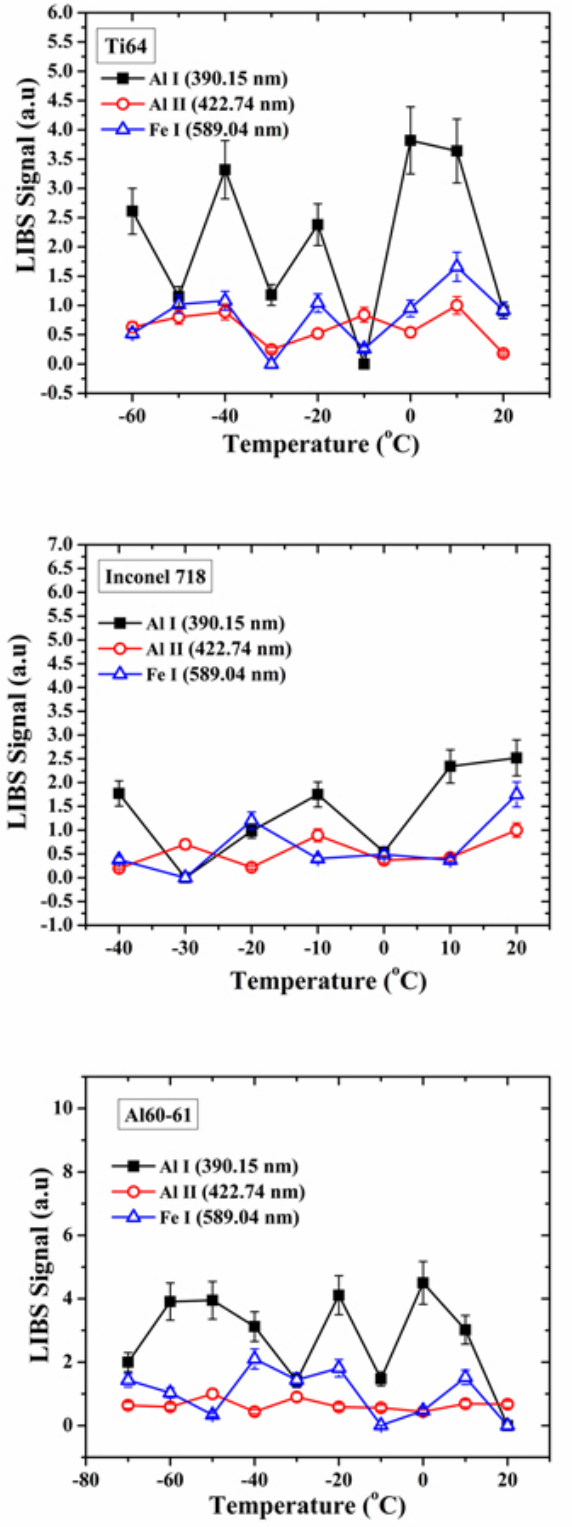

FIG. 5 Emitted intensity of spectral peaks as a function of the sample temperature.

of Eq. (3). In other words, the intensity of spectral emitted lines is related to the corresponding energy level population of the plasma species. The spectroscopic parameters like g_m, A_{mn}, and E_m can be retrieved from the available database. The atomic lines of Al I, Fe I, Cr I, Ni I elements are used to determine the electron temperature. A typical Boltzmann plot at sample temperature of 200°C is shown in Figure 7. In this figure, a linear fit and the experimental data are illustrated. From this plot, the electron temperature in Al 6061 alloy sample is obtained about 3206.56 K.

The profile of spectral line from LIBS technique has various broadening effects like Doppler broadening, Resonance broadening, and Stark broadening [31]. The Stark broadening is the dominant broadening in this technique. We have obtained the electron density from the flowing relation [32]:

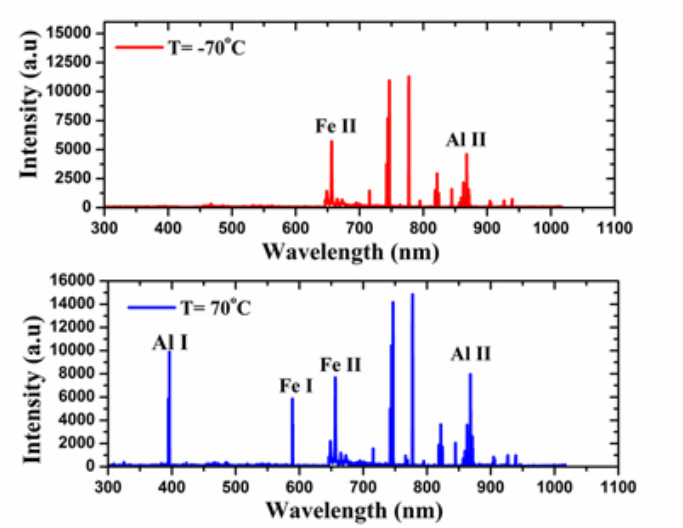

FIG. 6 A compression of spectra obtained at the temperatures of 70°C and (-70°C). Al I: 396.15 nm, Al II: 867.12 nm, Fe I: 588.93 nm, Fe II: 656.53 nm.

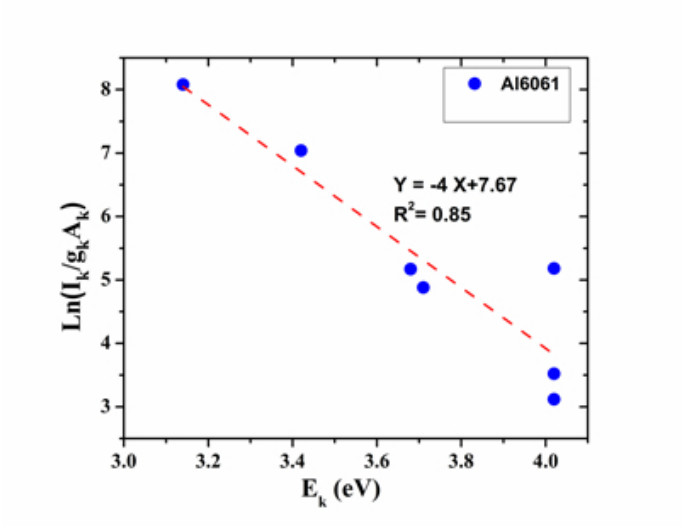

FIG. 7 Boltzmann plot obtained from the atomic spectral lines at sample temperature 200°C.

Specie	λ(nm)	g_kA_k ($\times10^7$ s^{-1})	E_k(eV)	$W_S(\times10^{-2}$ Å)
Al I	265,24	2,66	4,67	3,1
	308,21	25	4,02	
	309,27	44	4,04	
	396,15	20	3,14	
FE I	334,05	2,48	6,03	
	344,09	6,20	3,68	
	346,58	3,57	3,71	
	347,54	4,88	3,68	
	370,55	2,25	3,42	
Cr I	259,18	45	5,85	
	272,65	52	5,53	
	278,06	98	5,53	
	288,92	59	5,36	
	298,86	36	5,13	
Ni I	234,55	156,7	6,33	
	300,24	63,2	4,19	
	305,08	54,3	4,12	
	314,41	34,7	4,20	

TABLE 1 Spectroscopic parameters of the Al I, Fe I, Cr I, Ni I The data are taken from references [28, 30].

$$\Delta\lambda_s = 2\omega(n_e/10^6) \quad (4)$$

Where, n_e is the electron density in (cm^{-3}), $\Delta\lambda_s$(Å) is the FWHM of the Lorentzian line fit and ω is the electron impact parameter. In the LIBS signal, the line shapes are often fitted with a pure Lorentzian distribution, $\Delta\lambda_{fit}$. The spectrometer has a Gaussian instrumental line shape ($\Delta\lambda_{ins}$), so the Lorentzian Stark line width is then determined by:

$$\Delta\lambda_s = \left(\Delta\lambda_{fit}^2 - \Delta\lambda_{ins}^2\right)^{\frac{1}{2}} \quad (5)$$

$\Delta\lambda_{ins}$ was determined to be 0.37 nm by using Mercury-Argon calibration lamp (ACC-LK-HGAR-OCE, ANDOR, Ireland). A Lorentzan fit used for the determination of the electron density is shown in Figure 8. From this figure, the FWHM is obtained to be $\Delta\lambda_{fit} = 0.41$ nm.

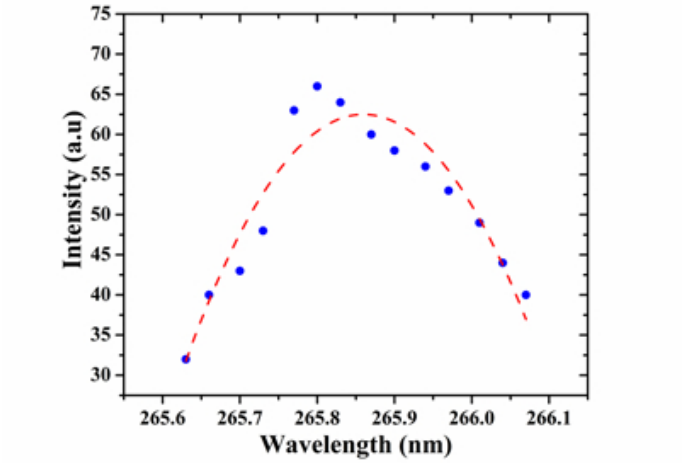

FIG. 8 Lorentzian fit for Al I: 265.80 nm spectral line at Al6061 alloy sample temperature 200 °C.

The evaluation of electron temperature and electron density via variation of sample temperature is shown in Figure 9. As can be seen, these parameters are temperature dependent. Decrease in collisions and energy transfer in cooling sample reduce electron temperature and electron density.

The electron temperature and electron density were calculated by LTE assumption, so it was necessary to confirm the validity of this assumption. According to McWhirter criterion [33], for the plasma to reach the state of LTE, the electron density n_e (cm^{-3}) should pass a threshold :

$$n_e \geq 1.6 \times 10^{12} T^{\frac{1}{2}} (\Delta E)^2 \quad (6)$$

Where, $\Delta E(eV)$ is the largest electronic transition considered and $T(K)$ is the electron temperature. In the present study, the largest transition corresponding to the observed line (the neutral aluminum line at 265.80 nm) was $\Delta E \approx 4.7$ eV. For temperatures approximately varying from -78°C to 200°C, the minimum density required for LTE condition between

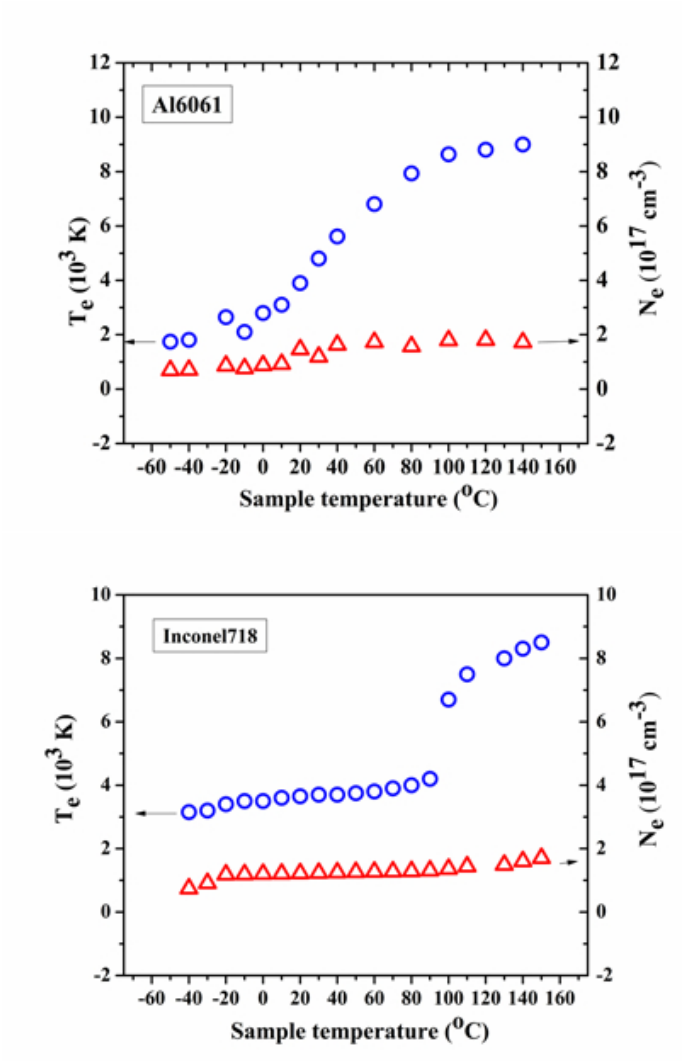

FIG. 9 Emitted intensity of spectral peaks as a function of the sample temperature.

17 - 40×10^{15}cm^{-3}, and 11- 40×10^{15}cm^{-3} for Inconel 718, and Al 6061, respectively. Clearly, the density measured here is always greater than the minimum density required by Eq. (4).

4 CONCLUSION

The effect of sample temperature on improvement of LIBS signal of Inconel 718, Titanium 64, and Aluminum 6061 was experimentally investigated. To our knowledge, this study is the first research about the effect of cooling samples on LIBS spectrum, especially on super alloys. The results showed increasing the sample temperature leads to improvement in the intensity of spectral lines as shown in other works [17, 18]. Increase in ablation rate can be the reason for this behavior. Fluctuations behavior and damping of some peaks are seen in cooling samples. These results suggested that cooling the sample temperature might decrease the intensity of LIBS signal. This effect can be attributed to the reduction of ablation rate and collisions between species. The electron density and the electron temperature are sensitive to sample temperatures.

References

[1] A. W. Miziolek, V. Palleschi, and I. Schechter, *Laser-Induced Breakdown Spectroscopy (LIBS), Fundamentals and Applications* (Cambridge University Press, Cambridge, 2006).

[2] R. Noll, *Laser-Induced Breakdown Spectroscopy, Fundamentals and Applications* (Springer, New York, 2012).

[3] G. Cristoforetti, A. D. Giacomo, M. Dell'Aglio, S. Legnaioli, E. Tognoni, V. Palleschi, et al., "Local thermodynamic equilibrium in laser-induced breakdown spectroscopy: Beyond the Mc Whirter criterion," Spectrochim. Acta B **65**, 86–95, (2010).

[4] D. A. Cremers, and L. J. Radziemski, *Handbook of Laser-Induced Breakdown Spectroscopy* (John Wiley & Sons, Haboken, 2006).

[5] J. P. Singh, and S. N. Thakur, *Laser Induced Breakdown Spectroscopy* (Elsevier, Amsterdam, 2007).

[6] S. Z. Mortazavi, P. Parvin, M. R. M. Pour, A. Reyhani, A. Moosakhani, and S.Moradkhani, "Time-Resolved evolution of metal plasma induced by Q-Switched Nd:YAG and ArF-excimer laser," Opt. Laser Technol. **62**, 32–39 (2014).

[7] V. Bulatov, R. Kransniker, and I. L. Schechter, "Converting spatial to pseudo resolution in laser plasma analysis by simultaneous multifiber spectroscopy," Anal. Chem. **12**, 2987–2994 (2000).

[8] L. Yaoming, J. Spenczak, and R. J. Gordon, "Nanosecond polarization-resolved laser-induced breakdown spectroscopy," Opt. Lett. **35**, 112–114 (2010).

[9] A. E. Majd, A. S. Arabanian, and R. Massudi, "Polarization resolved laser induced breakdown spectroscopy by single shot nanosecond pulsed Nd:YAG laser," Opt. Laser. Eng. **48**, 750–753 (2010).

[10] G. Cristoforetti, S. Legnaioli, V. Palleschi, A. Salvetti, and E. Tognoni, "Effect of target composition on the emission enhancement observed in double-pulse laser induced breakdown spectroscopy," Spectrochim. Acta B **63**, 312–323 (2008).

[11] V. N. Rai, J. P. Singh, F. Y. Yueh, and R. L. Cook, "Study of optical emission from laser-produced expanding across an external magnetic field," Laser Part. Beams **21**, 65–71 (2003).

[12] S. Palanco, L. M. Cabalin, D. Romero, and J. J. Laserna, "Infrared laser ablation and atomic emission spectrometry of stainless steel at high temperatures," J. Anal. Atom. Spectrom. **14**, 1883–1887 (1999).

[13] S. H. Tavassoli, and A. Gragossian, "Effect of sample temperature on laser-induced breakdown spectroscopy," Opt. Laser. Eng. **41**, 481–485 (2009).

[14] J. Scaffidi, W. Pearman, J. Chance, J. Carter, B. W. Colston, and S. Angel, "Effects of sample temperature in femtosecond single-pulse laser-induced breakdown spectroscopy," Appl. Optics **43**, 2786–2790 (2004).

[15] C. F. Su, S. Feng, J. P. Singh, F.-Y. Yueh, I. I. I. J. T. Rigsby, D. L. Monts, et al., "Glass composition measurement using laser induced breakdown spectrometry," Glass Technol. **41**, 16–21 (2000).

[16] C. Lopez-Moreno, K. Amponsah-Manager, B. W. Smith, I. B. Gornushkin, N. Omenetto, S. Palanco, et al., "Quantitative analysis of low-alloy steel by microchip laser induced breakdown spectroscopy," J. Anal. Atom. Spectrom. **20**, 552–556 (2005).

[17] R. Sangines, H. Sobral, and E. Alvarez-Zauco, "The effect of sample temperature on the emission line intensification mechanism in orthogonal double-pulse laser induced breakdown spectroscopy," Spectrochim. Acta B **68**, 40–45 (2012).

[18] C. Hanson, S. Phongikaroon, and J. R. Scott, "Temperature effect on Laser-induced breakdown spectroscopy spectra of molten and solid salts," Spectrochim. Acta B **97**, 76–85 (2014).

[19] S. Eschlbock-Fuchs, M. J. Haslinger, A. Hinterreiter, P. Kolmhofer, N. Huber, R. Rossler, et al., "Influence of sample temperature on the expansion dynamics and the optical emission of laser-induced plasma," Spectrochim. Acta B **87**, 36–42 (2013).

[20] S. Z. Shoursheini, P. Parvin, B. Sajad, and M. A. Bassam, "Dual-Laser-Beam-Induced Breakdown Spectroscopy of Copper using simultaneous continuous wave CO2 and Q-Switched Nd:YAG lasers," Appl. Spectrosc. **63**, 423–429 (2009).

[21] M. Aghaei, S. Mehrabian, and S. H. Tavassoli, "Simulation of nanosecond pulsed laser ablation of copper samples: A focuse on laser induced plasma radiation," J. Appl. Phys. **104**, 053303–053309 (2008).

[22] S. Palanco, L. M. Cabalin, D. Romero, and J. J. Laserna, "Infrared laser ablation and atomic emission spectrometry of stainless steel at high temperatures," J. Anal. Atom. Spectrom. **14**, 1883–1887 (1999).

[23] Material Properties Data, http://matweb.com/search/datasheet.aspx.

[24] D. Bauerl *Laser Processing and chemistry* (Springer, Berlin / Heidelberg, 2000).

[25] Refractive Index Database, http://Refractiveindex.info/legacy/.

[26] B. Salle, J. L. Lacour, P. Mauchien, P. Fichet, S. Maurice, and G. Manhes, "Comparative studies of different methodologies for quantitative rock analysis by Laser-Induced Breakdown Spectroscopy in a simulated Martian atmosphere," Spectrochim. Acta B **61**, 301–313 (2006).

[27] A. Ciucci, M. Corsi, V. Palleschi, S. Rastelli, A. Salvetti, and E. Tognoni, "New Procedure for quantitative element analysis by laser-induced plasma spectroscopy," Appl. Spectrosc. **53**, 960–964 (1999).

[28] NIST atomic spectra database, http://physics.nist.gov/physRefdata/ASD/.

[29] KURUCZ atomic spectral line database, http://www.pmp.uni-hannover.de/cgi-bin/ssi/test/kurucz/sekur/sekur.html.

[30] H. R.Griem, *Spectral Line Broadening by Plasmas. New York and London: A Subsidiary of Harcourt Brace Jovanovich* (Academic Press, New York, 1974).

[31] W. Demtroder *Laser Spectroscopy* (Springer, Heidelberg, 2008).

[32] G. Bekefi, C. Deutsch, and B. Yaakobi, *Spectroscopic Diagnostics of Laser Plasmas* (John Wiley and Sons, New York, 1976).

[33] M. Sabsabi, and P. Cielo, "Quantitative analysis of aluminum alloys by laser-induced breakdown spectroscopy and plasma characterization," Appl. Spectrosc. **49**, 499–507 (1995).